Effect of neutron halos on excited states of nuclei

A. A. Ogloblin,[1] A. N. Danilov,[1] T. L. Belyaeva,[2] A. S. Demyanova,[1] S. A. Goncharov,[3] and W. Trzaska[4]

[1]*RRC Kurchatov Institute, Moscow RU-123182, Russia*
[2]*Universidad Autonoma del Estado de Mexico, Codigo Postal 50000, Toluca, Mexico*
[3]*Moscow M. V. Lomonosov State University, Skobeltsyn Institute of Nuclear Physics, Moscow 119991, Russia*
[4]*Department of Physics, University of Jyväskylä, Survontie 9, FI-40500 Jyväskylä, Finland*

The differential cross sections of the inelastic scattering leading to the excitation of short-lived states in the stable ^{13}C and ^{9}Be nuclei as well as the radioactive ^{11}Be nucleus have been analyzed. Signatures of neutron halos in the excited states located close to the neutron emission thresholds have been investigated by applying a recently developed modified diffraction model. The abnormally large rms radius was identified for the 3.089-MeV $1/2^+$ state of ^{13}C. Significantly enlarged diffraction radii were found for the 1.68-MeV $1/2^+$ and the 3.05-MeV $5/2^+$ states of ^{9}Be. The analysis of the diffraction radii of the weakly bound radioactive ^{11}Be nuclei have shown that the 1.78-MeV $5/2^+$ and 3.41-MeV $3/2^+$ states in ^{11}Be have the same diffraction radii as the $1/2^+$ ground state, which is known as the best example of a state with one-neutron halo.

PACS number(s): 21.10.Gv, 24.10.Ht, 25.55.Ci, 25.60.Bx

I. INTRODUCTION

One of the most remarkable discoveries in nuclear physics from the end of the past century was the observation of neutron halos in some neutron-rich light nuclei [1]. The very term *exotic nuclei* was originally applied to nuclei possessing neutron halos [2]. This phenomenon manifests itself in the existence of a dilute surface region containing only neutrons (typically one or two) around a core with normal nuclear density. Formation of nuclear states located near the neutron emission thresholds and possessing enhanced radii was predicted long ago [3]. The physical reason of this effect is weak binding energy between the valence neutrons and the core, leading to long "tails" of their wave functions and consequently to an enhancement of nuclear radius. The effect is expected to be especially prominent for the neutrons occupying the s orbit, because in this case a centrifugal barrier is absent. The average distance between the valence neutrons and the center of the nuclear core in two-component nuclei such as ^{11}Be, ^{11}Li, and ^{14}Be can reach up to 7 fm [4,5], that is, about three times larger than their rms radii.

Neutron halos have been almost exclusively observed in ground states (g.s.) of some neutron-rich radioactive nuclei located close to the neutron drip line. Nevertheless, ideas about universality of the halo phenomenon were expressed soon after its discovery (see, e.g., Refs. [6,7]). Namely, Otsuka *et al.* held: "The neutron halo should not be limited to exotic nuclei and should be seen in excited states of large number of nuclei on and off the β-stability line, for instance, the first $1/2^+$ state of ^{13}C" [7]. Apparently, the observation of halos in the first excited states ($1/2^+$, $E_x = 3.089$ MeV) of ^{13}C and ^{12}B (1^-, $E_x = 2.62$ MeV) was first reported by Liu *et al.* [8], who employed the asymptotic normalization coefficient (ANC) method to estimate the radii of these states. The identities of some properties of halos in the ground states of the neutron-rich nuclei and those in the excited states of the stable nuclei were discussed in Ref. [9].

Observation of halos in the excited states can drastically extend the existing knowledge about exotic states of nuclei,

because some new features of nuclear structure might become apparent. The main reason why there was no search for halos in the excited states was the absence of reliable methods for measuring the radii of the short-lived ($\tau_{1/2} \lesssim 10^{-10}$ s) nuclear states. Indirect and usually nonquantitative information sometimes can be obtained from the nuclear form factors [10]; in particular, in Ref. [11] the analysis of the Hoyle state in ^{12}C was carried out by inelastic electron scattering.

Recently [12–15], we proposed a modified diffraction model (MDM) for determining the nuclear radii for such short-lived excited states and applied it to determine the rms radii of ^{12}C in the excited states lying near and above the α-particle breakup threshold. Our approach allowed us to determine the enhanced radius of the famous Hoyle state (0_2^+, $E_x = 7.65$ MeV), and it seems to be an effective method to study cluster and α-condensation properties of light nuclei, which received the bulk of attention in recent years [16–19]. It is challenging to extend this method to the states of the light stable nuclei located close to the neutron emission thresholds, especially to those where the existence of neutron halos could be expected. Besides determining the nuclear sides in the excited states below the neutron emission threshold, such a study would provide additional information that could be useful for further development of the method. One application of the MDM relates to determining the diffraction radii for some short-lived states located above the neutron emission threshold in order to look for theirenhancement.

In this paper, the MDM is applied to determine the diffraction radii of the $1/2^+$ states of ^{13}C and ^{9}Be from the existing data of the inelastic ^{3}He- and α-particle scattering. The data of ^{11}B $+^{12}$C scattering are analyzing with the aim to extract the diffraction radii of ^{11}B in the $5/2^+$ and $3/2^+$ states that are the members of the $1/2^+$ g.s. band in ^{11}B.

II. MODIFIED DIFFRACTION MODEL

A diffraction scattering model [20], a fairly rough approximation for calculating the differential cross sections, is

adequate to determine nuclear radii from experimental data. Its advantage consists in operating with a single parameter having the dimension of length, the diffraction radius, which is directly determined from the positions of the minima (maxima) of the experimental angular distributions. In more accurate approaches, for example, the optical model, the nuclear radius manifests in an implicit and ambiguous manner in the parameters of the real and imaginary parts of the optical potential, which in turn are determined by fitting the calculations to the measured cross sections; therefore, these depend on the quality of both the fit and the data.

The adiabatic approximation, which is used in the diffraction model, implies freezing a target nucleus during a collision. Because of this, inelastic scattering is replaced by elastic scattering that takes place on the nuclear surface modified in the process of forming the excited state. Accordingly, the total reaction amplitude consists of two parts. One describes the elastic scattering on a black disk, corresponding to the initial state, and the second corresponds to the additional elastic scattering, which is a contribution from the edge. As a result, the differential cross sections are described by the squares of the cylindrical Bessel functions of various orders from the argument proportional to some radial parameter R_{dif} (diffraction radius), which depends on both nuclear structure and interaction dynamics. If a diffraction radius is conserved in the elastic and inelastic scattering, then certain phase relations (so-called Blair phase rules) between the angular distributions of the elastic and inelastic scattering appear [20]. Because these relations are fulfilled very well in many cases of inelastic scattering with excitation of levels at which one should expect constant real nuclear radii (e.g., for the lowest members of the rotational band), the deviations from it can serve as an indicator of changes in the size of a nuclear state.

We have developed a modified diffraction model [12–14], which assumes that the rms $\langle R^* \rangle$ radius of the excited state can be determined by the difference of diffraction radii of the excited and the ground states using the following relations:

$$R_{dif}^0(el) = \langle R_0 \rangle + \langle R_1 \rangle + \Delta_{el}, \qquad (1)$$

$$R_{dif}^*(in) = \langle R^* \rangle + \langle R_1 \rangle + \Delta_{in}, \qquad (2)$$

$$\langle R^* \rangle = \langle R_0 \rangle + \left[R_{dif}^*(in) - R_{dif}^0(el) \right] + (\Delta_{el} - \Delta_{in}). \qquad (3)$$

Here $\langle R_0 \rangle$ and $\langle R_1 \rangle$ are the rms matter radii of the colliding nuclei in their ground states, which are assumed to be known. Namely, it is assumed that the rms matter radius of the "normal" nucleus coincides with the radius of the proton distribution in the nucleus (i.e., the radius of the matter distribution of neutrons in the nucleus coincides with the radius of the proton distribution), $\langle R_0 \rangle = \sqrt{\langle R^2 \rangle_p}$. The matter radius of the proton distribution in the nucleus can be estimated (see, e.g., [21] with reference to the book [22]) as

$$\langle R^2 \rangle_p = \langle R^2 \rangle_{ch} - 0.77 + 0.11 N/Z.$$

The values of rms charge radii of the nuclei $\langle R^2 \rangle_{ch}$ are taken from Ref. [23]. $R_{dif}^*(in)$ and $R_{dif}^0(el)$ are the diffraction radii determined from the positions of the minima and maxima of the experimental angular distributions of the inelastic and elastic scattering, respectively. Parameters Δ_{el} and Δ_{in} represent the difference between the diffraction radii and the
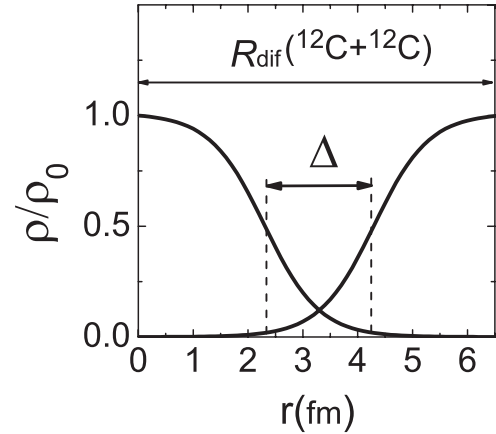

FIG. 1. Schematic view of the density superposition of the colliding ^{12}C nuclei in the elastic diffraction scattering. The vertical dashed lines correspond to the rms radii of the colliding nuclei.

sum of "true" (e.g., rms) radii of the nuclear states involved in the reactions (Fig. 1), and thus they determine the distance to which the colliding nuclei must approach to evoke a diffraction. Values of Δ include all the structural and dynamic effects that are neglected in the diffraction model. For the elastic scattering, the Δ_{el} value can be determined directly from experimental data. Energy dependence of Δ_{el} in the c.m. system for various combinations of colliding nuclei was shown in Fig. 5 of Ref. [13].

A common feature of Δ_{el} values is their monotonic decrease with energy, meaning that diffraction occurs at a stronger overlap of nuclear densities as the energy increases. Such behavior correlates with the known fact that the diffraction radius is close to the strong absorption radius. We also note that for the projectiles with lower average densities (deuterons, ^{6}Li), diffraction takes place at a smaller distance between the colliding nuclei.

To determine the radius of a nucleus in the excited state, we should make some assumptions about a behavior of unknown quantities Δ_{in}. Though it cannot be strictly justified, it is reasonable to suggest that Δ_{in} and Δ_{el} are similar in their main aspects. In Refs. [12–14], we used

$$\Delta_{in} = \Delta_{el}. \qquad (4)$$

This means that the radius of the excited state is determined in MDM not absolutely, but relative to the radius of the ground state by adding the difference of both diffraction radii. One of the arguments in favor of Eq. (4) is that the Blair phase rules have been confirmed by numerous examples to be valid, as mentioned previously.

Applications of the MDM for the inelastic scattering of ^{2}H, ^{3}He, ^{4}He, ^{6}Li, and ^{12}C on ^{12}C in a wide range of energies allowed us to get consistent values of the rms radii of ^{12}C in several levels for which enlarged sizes were expected. In particular, we showed that the Hoyle state, in line with the expectations, really has an abnormally large radius. The results were confirmed by another independent method that used the inelastic rainbow scattering of ^{3}He and ^{4}He on ^{12}C [12,14]. In addition, the analysis of the available data of the inelastic scattering from ^{11}B and ^{13}C [24] has shown that the spectra

of these nuclei also contain the α-cluster states with extended sizes, which can be considered as the analogs of the Hoyle state.

In this study, we use the MDM to determinate the radii of the nuclear states, for which we expect the existence of a neutron halolike structure. Of course, we do not argue in advance that Eq. (4) remains valid for nuclei with very different distributions of the nucleon density or that it will not depend on energy.

III. DETERMINATION OF THE DIFFRACTION RADII

A. Diffraction radii for the excited states of ^{13}C

The first $1/2^+$ excited state of ^{13}C at $E_x = 3.089$ MeV is located 1.86 MeV below the ^{12}C + n threshold. Determination of its radius with the MDM has a special significance for the method in general, because it allows us to compare our results with those obtained by an independent approach [8] (the ANC method).

The available data of the ^{3}He + ^{13}C inelastic scattering at $E_{c.m.} = 30$–40 MeV [25–28], as well as the $\alpha = ^{13}$C inelastic scattering at similar energies [29,30] and at 388 MeV [31], are explored for the diffraction analysis. Figure 2(a) shows an example of the differential cross sections of the ^{3}He + ^{13}C elastic and inelastic scattering. According to the Blair phase rule, the elastic and inelastic (to $1/2^+$ state) angular distributions should be in phase. However, Fig. 2(a) shows that the minima and maxima positions of the inelastic cross section are systematically shifted toward the smaller angles with respect to their corresponding positions in the elastic angular distribution. This fact is a signature [12,13,32] of the increased diffraction radius of the $1/2^+$ state.

The diffraction radii at each specific energy are determined by averaging the data obtained from the positions of several minima and maxima at small angles, which are identified
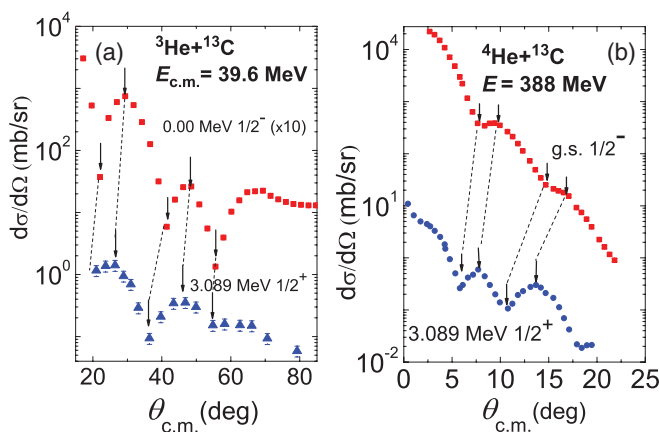

FIG. 2. (Color online) Differential cross sections of the (a) ^{3}He + ^{13}C and (b) ^{4}He + ^{13}C elastic [25] and inelastic [26] scattering at $E(^3$He$) = 39.6$ MeV and $E(^4$He$) = 388$ MeV [31]. The shift toward smaller angles of the minima and maxima positions in the inelastic scattering relatively to those in the elastic cross sections is clearly seen. The arrows in this and the following figures indicate the minimum and maximum positions used to determine the diffraction radii.
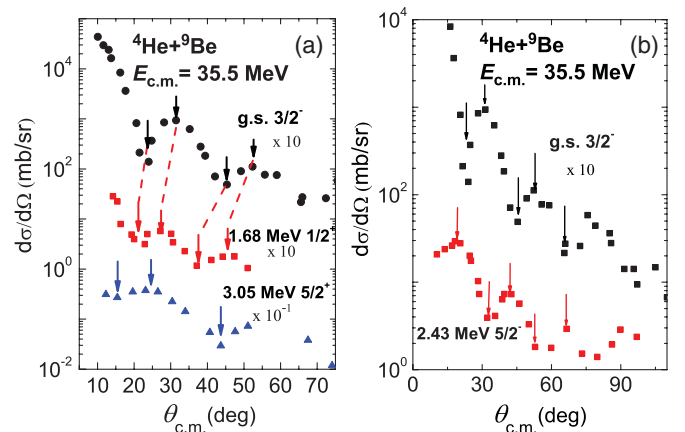

FIG. 3. (Color online) Differential cross sections of the inelastic ^{4}He + ^{9}Be scattering at 35.5 MeV leading to the excitation of the lowest ^{9}Be states with (a) positive parity: 1.68-MeV $1/2^+$ and 3.05-MeV $5/2^+$ states and (b) negative parity: 0.00-MeV $3/2^-$ and 2.43-MeV $5/2^-$ states. Data are from Ref. [33]. The shift mentioned in the caption of Fig. 2 is seen for the positive parity levels and absent for the negative ones.

as extremes of the squared Bessel functions. Normally, the positions of 2–3 minima and maxima are used for the analysis as shown in Figs. 2 and 3. More details about the procedure are given in Ref. [13]. In the most cases, deviations from the average values do not exceed 0.10 fm. The energy-averaged differences $(R_{\text{dif}}^* - R_{\text{dif}}^0)$ of the diffraction radii between the 3.089-MeV $1/2^+$ state and the ground state are 0.53 ± 0.12 fm for the α-particle scattering and 0.40 ± 0.07 fm for the ^{3}He scattering in the low-energy region. The diffraction radius of the 3.089-MeV state determined from the α-particle scattering at $E_\alpha = 388$ MeV [31] [Fig. 2(b)] is also found to be larger than that for the ground state.

The diffraction radii for the other excited states located between the 3.089-MeV level and the cluster states, analogs of the Hoyle state (see Ref. [24]), are identical with the diffraction radius of the ground state within the error bars. This fact confirms the exceptional character of the 3.089-MeV $1/2^+$ state of ^{13}C.

B. Diffraction radii for the excited states of ^{9}Be

This nucleus has two well-developed rotational bands of different parities based on the ground and first excited states, correspondingly. The first three states in the π band are g.s. $3/2^-$, 2.43-MeV $5/2^-$, and 6.38-MeV $7/2^-$ states. The four lowest states in the σ band are 1.68-MeV $1/2^+$, 3.05-MeV $5/2^+$, 4.70-MeV $3/2^+$, and 6.76-MeV $9/2^+$. We analyze the existing scattering data: $\alpha + ^9$Be at 35.5, 50, and 65 MeV, and ^{3}He + ^{9}Be at 50 MeV [33–35]. They all contain the elastic and inelastic (with excitation of the 2.43-MeV $5/2^-$ state) differential cross sections. Transitions to some positive parity levels were measured only for the $\alpha + ^9$Be scattering at 35.5 MeV [33]. The differential cross sections of the elastic and inelastic (to the 1.68-, 2.43-, and 3.05-MeV states) scattering are shown in Fig. 3(a).

TABLE I. Diffraction radii of ^{9}Be in the excited states obtained from the analysis of the scattering data.

E_x (MeV), J^π	R_{dif} (fm)[a]
0.00, $3/2^-$	5.18 ± 0.03
1.68, $1/2^+$	6.38 ± 0.14
2.43, $5/2^-$	5.25 ± 0.05
3.05, $5/2^+$	> 6.3
6.38, $7/2^-$	5.27 ± 0.13

[a]The diffraction radii of $3/2^-$ and $5/2^-$ states are obtained by averaging the data of the α particle and ^{3}He scattering at different energies.

The systematical shift of the minimum and maximum positions of the inelastic angular distribution corresponding to the formation of the 1.68-MeV $1/2^+$ state with respect to the elastic-scattering cross section is observed, which clearly indicates the difference of the diffraction radii for the first excited and the ground states. On the other hand, no significant deviations from the Blair rules are seen in the cross sections corresponding to the transitions to the negative parity levels, as one can see from Fig. 3(b).

The extracted diffraction radii for the lowest states of ^{9}Be are shown in Table I. For the ground and the 2.43-MeV states, the values of R_{dif} practically do not depend either on the energy or the type of the projectiles. As the doublet, 6.38-MeV $7/2^-$ and 6.76-MeV $9/2^+$ were not resolved in the data of Ref. [33], and we attributed the spin-parity value $7/2^-$ to the whole group. [An argument in favor of such a choice is the much larger cross section of the transition to the $5/2^-$ state in comparison with that to the $5/2^+$ one; see Figs. 3(a) and 3(b).] The value of the corresponding diffraction radius is close to those obtained for other two members of the π band.

The diffraction radii for the two states with positive parity, the members of the σ band, are significantly ($\sim$1 fm) larger.

Thus, from the inelastic scattering data, it follows that the lowest excited states with $J^\pi = 1/2^+$ in the ^{13}C and ^{9}Be have abnormally large diffraction radii.

IV. DISCUSSION

A. Neutron halo in the excited state of ^{13}C

Because the MDM has no strict theoretical foundation and is based on empirical systematics, we should compare the results obtained within this model with the data for some reference excited state with a known "true" radius. In the case of the threshold α-cluster states, we refer to the Hoyle state, which is known to have a larger size. Applicability of the MDM and, in particular, Eq. (4) was demonstrated in the detailed and consistent studies of the diffraction radius dependences from the energy and different types of incident particles and was confirmed by independent rainbow scattering analysis [12–14]. It is difficult to analyze the neutron halo in the excited states because of the lack of experimental data. The only object with which it is possible to make a comparison is the first excited state of ^{13}C. According to Eqs. (1)–(3), the rms radius of ^{13}C in the 3.089-MeV $1/2^+$ excited state

determined from the analysis of the data at low energies (at $E_{c.m.} \simeq 40$ MeV, the average value of $R^*_{dif} = 5.97$ fm) is found to be $\langle R^* \rangle = 2.74 \pm 0.06$ fm. This value is about 0.4 fm larger than the rms radius of ^{13}C in its ground state, $\langle R_0 \rangle = 2.33$ fm. The increased rms radius does not automatically mean the appearance of a halo, but a natural explanation of such enhancement in this particular case is that the s-state wave function of the valence neutron has asymptotically a long exponential "tail" $\exp(-kr)$, which strongly increases the probability for the neutron to be outside the ^{12}C core. The corresponding length parameter $1/k = (\mu\varepsilon)^{-1/2}$ is equal to 3.5 fm, which gives a rough estimation of the average distance between a neutron and the ^{12}C core (i.e., the halo radius):

$$R_h(^{13}C) = \langle R(^{12}C) \rangle + 1/k = 5.8 \, \text{fm}. \quad (5)$$

This estimate implies that the 3.089-MeV $1/2^+$ excited state is a single-particle one. An argument in favor of this suggestion follows from an analysis of the ^{12}C$(d,p)^{13}$C reaction. The spectroscopic factors for the $1/2^-$ g.s. and the 3.089-MeV $1/2^+$ and 3.85-MeV $5/2^+$ excited states have large values: 0.77, 0.65, and 0.58, respectively [36], in accordance with their expected single-particle nature.

Using a more accurate expression for the radius of a one-neutron halo from Ref. [37],

$$(A + 1)\langle R^2 \rangle_{(A+1)} = A\langle R^2 \rangle_A + [A/(A + 1)]R_h^2, \quad (6)$$

we obtain $R_h(^{13}C) = 5.88 \pm 0.39$ fm, which is in good agreement with the estimate given previously.

Calculations of the matter-density profiles [6] of ^{13}C in the $1/2^+$ excited state and ^{11}Be in the $1/2^+$ halo ground state demonstrated their similarity (see Fig. 2 in Ref. [6]). We find that $R_h(^{13}C)$ is a little smaller than the halo radius of ^{11}Be in the $1/2^+$ ground state, $R_h = 6.65$ fm. This is reasonable, because the binding energy of the valence neutron in ^{11}Be is 0.5 MeV, versus 1.86 MeV for ^{13}C.

The ^{13}C nucleus was examined in Ref. [8], where an analysis of the ^{12}C$(d,p)^{13}$C cross section at 12 MeV within the ANC approach led to the conclusion that a neutron halo should exist in the 3.089-MeV $1/2^+$ excited state of this nucleus. The extracted value of the halo radius, $R_h(^{13}C) = 5.04 \pm 0.75$ fm calculated in Ref. [8], is similar to our result (within the error bars).

The criteria for a halo formation have been explored in a number of studies. The most stringent of them [38],

$$B_n A^{2/3} < 2 \, \text{MeV}, \quad (7)$$

where B_n is the binding energy of the valence neutron, is not fulfilled even for the ground state of ^{11}Be. A more benign condition [38,39], which requires that the probability P of a neutron staying out of the potential should be larger than 50%, suggests

$$B_n A^{2/3} < 10 \, \text{MeV}, \quad (8)$$

which agrees well with the available data. For the considered state of ^{13}C, $B_n A^{2/3} = 10.3$, and the probability $P = 55\%$ [39].

Thus, we can conclude from this analysis that ^{13}C in the 3.089-MeV $1/2^+$ state really has a neutron halo with a radius of between 5 and 6 fm.
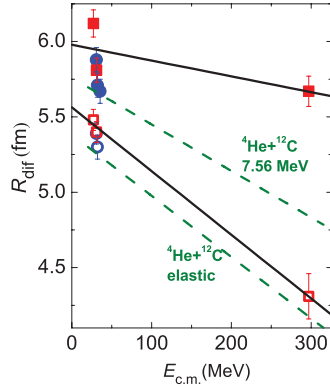
FIG. 4. (Color online) Energy dependence of the diffraction radii determined from the elastic (open symbols) and inelastic (filled symbols) scattering data for the $\alpha + {}^{13}C$ (squares) and ${}^{3}He + {}^{13}C$ (circles) systems; the energy dependences of R_{dif} from the elastic and inelastic (to the 7.56-MeV 0_2^+ state) $\alpha + {}^{12}C$ scattering [13] are shown by the dashed lines.

Based on this result, we conclude that the rms radius of this state determined by applying Eqs. (3) and (4) to the data at $E_\alpha = 388$ MeV is strongly overestimated, because it leads to an unrealistically large radius of the halo, $R_h = 10.5 \pm 0.9$ fm. The energy dependences of the diffraction radii for the elastic and inelastic scattering to the 3.089-MeV state scattering of ${}^{3,4}He$ on ${}^{13}C$ are shown in Fig. 4(a) and compared with the similar data for $\alpha + {}^{12}C$ scattering. The diffraction radii for the $\alpha + {}^{13}C$ elastic scattering behave in accordance with the previously established systematics. The solid line connecting their values at different energies runs parallel to similar lines, corresponding to both the elastic scattering of $\alpha + {}^{12}C$ and the inelastic one of the Hoyle state. The energy dependence of the diffraction radii for the inelastic $\alpha + {}^{13}C$ scattering is shown by a gently descending solid line in Fig. 4(a). Thus, these diffraction radii are smoothly reduced with energy rise, which indicates an increase of the $[R_{dif}^*(in) - R_{dif}^0(el)]$ difference with energy.

According to Eq. (3), the observed energy dependence of the $[R_{dif}^*(in) - R_{dif}^0(el)]$ difference means that the $(\Delta_{in} - \Delta_{el})$ difference also increases with energy. Consequently, at higher energies, $\Delta_{in} > \Delta_{el}$ and a diffraction in the inelastic channel occurs at larger distances than a diffraction in the elastic scattering. Note that a similar increase of the $[R_{dif}^*(in) - R_{dif}^0$ (el)] difference with energy was already observed in Ref. [13] for the inelastic $d + {}^{12}C$ scattering, leading to the excitation of the Hoyle state. Thus, the energy dependence of the diffraction radii in the inelastic scattering involving nuclear states with very low nucleonic densities may be different from that observed in "normal" cases. Alternatively, we cannot exclude the possibility of general inadequacy of the diffraction model at such high energies. A definite conclusion cannot be drawn because of the lack of data. The limits of application of Eq. (4) should continue to be studied in further investigations.

B. Comparison of the ⁹Be and ¹¹Be diffraction radii

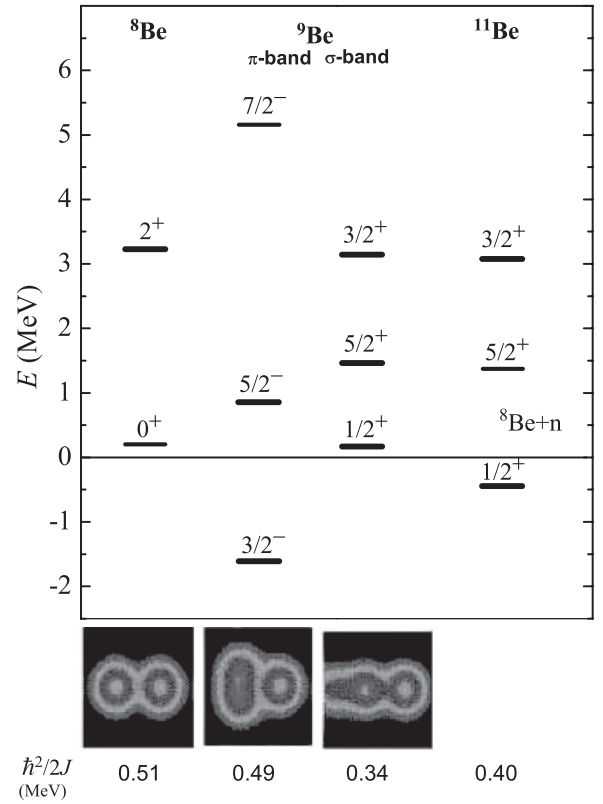Theory predicts that ⁹Be has a two-center $\alpha + \alpha + n$ quasimolecular structure with valence neutrons occupying π

FIG. 5. Rotational states of ⁸Be, ⁹Be ($K = 3/2^-$ and $K = 1/2^+$ bands) and ¹¹Be. In the lower panel, the AMD predictions for the neutron density distributions of Togashi *et al.* [40] are shown together with the inverse values of the moments of inertia.

and σ orbits (see, e.g., Ref. [19]) (Fig. 5). The ground state is only 1.67 MeV below the neutron emission threshold, even less than for the 3.089-MeV state in ¹³C. However, the rms radius of ⁹Be is equal to 2.39 fm, that is, similar to those of neighboring stable nuclei without any signatures of the existence of a halo [though condition (9) for its formation is fulfilled]. Antisymmetrized molecular dynamic (AMD) calculations [40] also do not predict an extended neutron density distribution for the ⁹Be ground state.

The first excited $1/2^+$ ($E_x = 1.68$ MeV) state is 20 keV above the neutron-decay threshold. It is a well-developed state with a long half-life ($\Gamma \approx 220$ keV) and well-established $\alpha + \alpha + n$ cluster structure [19,40], where the valence neutron occupies the s orbit. The diffraction radii for this state and for the second member of the σ band (3.05 MeV $5/2^+$) are significantly larger than the radii of the negative-parity states (see Table I). The lack of accuracy of the data concerning the excitation of the 3.05-MeV $5/2^+$ state allows us to make only a very rough estimate of its radius (Table I). However, the main result is that ⁹Be in this state retains the large diffraction radius in spite of the increase of the angular momentum by two units. The $[R_{dif}^*(in) - R_{dif}^0(el)]$ differences are approximately three times larger than these values for ¹³C. Remember that ⁹Be in the states of the σ band has the enhanced moment of inertia in comparison with the states of the π band (Fig. 5). The diffraction radii of levels belonging to the rotational π band of ⁹Be are the same (see Table I) regardless of whether

they are above or below the neutron threshold. The diffraction radii for negative states are ≈ 1.1 fm less that those for the states with positive parity.

Obviously, the scientific terms are defined as they first appear, and the term *halo* is introduced for the ground state of neutron-rich nuclei close to the drip line. An explanation of this phenomenon is usually associated with the long "tail" of the wave function of the valence neutron. Until now, the question of how to treat the enhanced nuclear structure in the above-threshold states was not considered, partly because of the evident difficulty of precise determining the "real" radius of a neutron unbound state in the continuum. Discussion of any theoretical aspects of the problem is outside the scope of this paper. We restrict this discussion to determining the diffraction radii of the states; the radii of the rotational states in continuum have not been measured previously.

It is worthwhile to compare the diffraction radii for the rotational σ band of ^{9}Be with the similar ones of ^{11}Be. We already pointed out that the ground $1/2^+$ state of ^{11}Be is the most striking example of an one-neutron halo. The excited 1.78-MeV $5/2^+$ and 3.41-MeV $3/2^+$ states, lying above the neutron emission threshold, form a rotational band with the parameters very close to the σ band of ^{9}Be (Fig. 5). The quasielastic and inelastic ^{11}Be + ^{12}C scattering leading to formation of the ground and both excited states of ^{11}Be (Fig. 6) has been measured in Refs. [41] and [42]. We are well aware that the analysis of these data within the MDM can be only qualitative (because of nonsystematic character of the data), but nevertheless we try to extract the diffraction radii for these states (see Table II).

We find that the diffraction radii for the previously mentioned excited states in ^{11}Be do not differ for the g.s. and are also sufficiently enlarged. Then, just as in the case of ^{9}Be, neither an increase of the angular momenta nor the possibility of decay by a neutron emission lead to a change of the diffraction radii. Because these above-threshold states belong to the rotational band, the angular momentum barrier can stabilize them against a neutron decay. The approximate equality of the diffraction radii for the ground (bound)
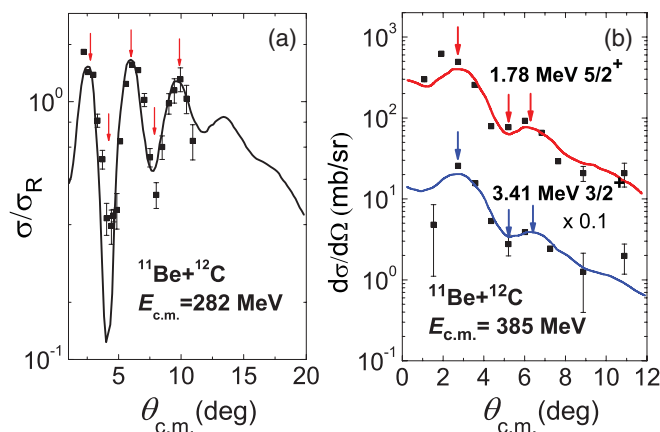
TABLE II. Diffraction radii for the ground and the excited states of ^{11}Be obtained from the analysis of the ^{11}Be + ^{12}C scattering data.

Reaction	$E_{\text{c.m.}}$ (MeV)	E_x (MeV)	J^π	R_{dif} (fm)	$R_{\text{dif}}^* - R_{\text{dif}}^0$ (fm)
^{11}Be + ^{12}C	282	0.00	$1/2^+$	5.60 ± 0.07	
	384	1.78	$5/2^+$	5.72 ± 0.17	0.12 ± 0.18
	384	3.41	$3/2^+$	5.77 ± 0.15	0.17 ± 0.17

and the excited (unbound) states suggests that these states have radii of equal rms. This suggestion requires additional theoretical studies, which, we hope, can be stimulated by our results determining the diffraction radii for the above-threshold excited states in ^{11}Be.

V. CONCLUSIONS

A modified diffraction model previously used for determining the radii of the exotic α-cluster states in ^{12}C [12–14] was used to analyze the ^{4}He and ^{3}He inelastic scattering on ^{13}C and ^{9}Be, leading to the excitation of states for which the existence of neutron halos might be expected. The rms radius of ^{13}C in the 3.09-MeV $1/2^+$ state located 1.86 MeV below the neutron emission threshold was found to be $\langle R \rangle = 2.74 \pm 0.06$ fm. It is significantly greater than the ^{13}C radii, in both the ground and the second excited 3.68-MeV $3/2^-$ states, even though the latter is located nearer to the ^{12}C + n threshold. Assuming that the $1/2^+$ state has a halo, we calculated its radius to be equal $R_h = 5.88 \pm 0.39$ fm. This value is consistent with the result of an independent analysis of ^{12}C$(d,p)^{13}$C data [8]. Comparison with the $1/2^+$ ground state of ^{11}Be showed clear similarity of the properties of both $1/2^+$ states; the slightly more developed halo in ^{11}Be is easily explained by the lower binding energy of the valence neutron.

The results concerning the $1/2^+$ state of ^{13}C demonstrated the applicability of MDM for measuring the radii of the nuclear states that are not cluster structures. However, the relation between the diffraction and the rms radii probably is more complicated than supposed earlier for the α-cluster states [12–14] and requires further investigation.

In spite of the difficulty of precisely determining the "real" radii of neutron-unbound states in the continuum, the determination of the diffraction radii for such states is a problem worthy of further examination. Thus, several states located above the neutron emission thresholds in ^{9}Be and ^{11}Be with the anomalously large diffraction radii were identified. The very large diffraction radius was determined for the 1.68-MeV $1/2^+$ state of ^{9}Be. For the next member of the σ band, the 3.05-MeV $5/2^+$ state, we also found the same enhanced diffraction radius. We found that ^{11}Be in the excited 1.78-MeV $5/2^+$ and 3.41-MeV $3/2^+$ states, lying above the neutron threshold, have diffraction radii approximately equal to that of the ground state. These levels have much in common with the positive parity band in ^{9}Be: the inverted sequence of the $5/2^+$ and $3/2^+$ states and similar enhanced moments of inertia. These states above the neutron emission threshold form the rotational band, so that the angular-momentum barrier stabilize them against neutron decay.

FIG. 6. (Color online) Differential cross sections of the ^{11}Be + ^{12}C scattering: (a) quasielastic scattering at $E_{\text{c.m.}} = 282$ MeV [41]; (b) inelastic scattering leading to the excitation of the 1.78-MeV $5/2^+$ and 3.41-MeV $3/2^+$ states of ^{11}Be at $E_{\text{c.m.}} = 385$ MeV [42].

[1] I. Tanihata *et al.*, Phys. Rev. Lett. **55**, 2676 (1985).

[2] P. G. Hansen and B. Jonson, Europhys. Lett. **4**, 409 (1987); B. Jonson, Phys. Rep. **389**, 1 (2004).

[3] A. I. Baz, Adv. Phys. **8**, 349 (1959); Sov. Phys.—JETP **36**, 1762 (1959).

[4] W. Nörtershäuser *et al.*, Phys. Rev. Lett. **102**, 062503 (2009).

[5] R. Sánchez *et al.*, Phys. Rev. Lett. **96**, 033002 (2006).

[6] T. Otsuka, N. Fukunishi, and H. Sagawa, Phys. Rev. Lett. **70**, 1385 (1993).

[7] T. Otsuka, M. Ishihara, N. Fukunishi, T. Nakamura, and M. Yokoyama, Phys. Rev. C **49**, R2289 (1994).

[8] Z. H. Liu *et al.*, Phys. Rev. C **64**, 034312 (2001).

[9] Z. H. Liu, X. Z. Zhang, and H. Q. Zhang, Phys. Rev. C **68**, 024305 (2003).

[10] A. A. Ogloblin, S. A. Goncharov, T. L. Belyaeva, and A. S. Demyanova, Phys. At. Nucl. **69**, 1149 (2006).

[11] M. Chernykh, H. Feldmeier, T. Neff, P. von Neumann-Cosel, and A. Richter, Phys. Rev. Lett. **98**, 032501 (2007).

[12] A. S. Demyanova, A. A. Ogloblin, S. A. Goncharov, and T. L. Belyaeva, Int. J. Mod. Phys. E **17**, 2118 (2008); A. S. Demyanova *et al.*, Phys. At. Nucl. **72**, 1611 (2009).

[13] A. N. Danilov, T. L. Belyaeva, A. S. Demyanova, S. A. Goncharov, and A. A. Ogloblin, Phys. Rev. C **80**, 054603 (2009).

[14] A. A. Ogloblin, T. L. Belyaeva, A. N. Danilov, A. S. Demyanova, and S. A. Goncharov, Nucl. Phys. A **834**, 143 (2010); AIP Conf. Proc. **1224**, 100 (2010).

[15] T. L. Belyaeva, A. N. Danilov, A. S. Demyanova, S. A. Goncharov, A. A. Ogloblin, and R. Perez-Torres, Phys. Rev. C **82**, 054618 (2010).

[16] A. Tohsaki, H. Horiuchi, P. Schuck, and G. Ropke, Phys. Rev. Lett. **87**, 192501 (2001).

[17] Y. Funaki, H. Horiuchi, W. von Oertzen, G. Ropke, P. Schuck, A. Tohsaki, and T. Yamada, Phys. Rev. C **80**, 064326 (2009).

[18] W. von Oertzen, Lect. Notes Phys. **818**, 109 (2010).

[19] W. von Oertzen, M. Freer, and Y. Kanada-En'yo, Phys. Rep. **432**, 43 (2006).

[20] J. S. Blair, in *Lectures in Theoretical Physics*, edited by F. D. Kunz, D. A. Lind, and W. E. Britten (University of Colorado Press, Boulder, 1966), Vol. 8.

[21] G. R. Satchler and W. G. Love, Phys. Rep. **55**, 183 (1979).

[22] R. C. Barrett and D. F. Jackson, *Nuclear Size and Structure* (Clarendon Press, Oxford, 1977).

[23] I. Angeli, At. Data Nucl. Data Tables **87**, 185 (2004).

[24] A. S. Demyanova, A. N. Danilov, A. A. Ogloblin, S. A. Goncharov, and T. L. Belyaeva, Int. J. Mod. Phys. E **20**, 915 (2011).

[25] A. S. Demyanova *et al.*, Phys. Scr. T **32**, 89 (1990).

[26] G. C. Ball and J. Cerny, Phys. Rev. **177**, 1466 (1969).

[27] G. Thiamova *et al.*, Nucl. Phys. A **697**, 25 (2002).

[28] R. J. Peterson, J. R. Shepard, and R. A. Emigh, Phys. Rev. C **24**, 826 (1981).

[29] S. V. Artemov *et al.*, Izv. Akad. Nauk. Ser. Fiz. **65**, 1579 (2001).

[30] B. G. Harvey *et al.*, Phys. Rev. **146**, 712 (1966).

[31] T. Kawabata *et al.*, Int. J. Mod. Phys. E **17**, 2071 (2008).

[32] S. Ohkubo and Y. Hirabayashi, Phys. Rev. C **70**, 041602(R) (2004); **75**, 044609 (2007).

[33] R. J. Peterson, Nucl. Phys. A **377**, 41 (1982).

[34] N. Burtebaev, A. Duisebaev, G. Ivanov, and V. Kanashevich, Nuclear Physics Institute Report NPI 88-01, Alma-Ata, Kazakhstan, 1988 (unpublished); V. V. Adodin, N. T. Burtebaev, and A. D. Duisebaev, Yad. Fiz. **55**, 577 (1992) [Sov. J. Nucl. Phys. **55** (1992)].

[35] S. Roy, J. M. Chatterjee, H. Majumdar, S. K. Datta, S. R. Banerjee, and S. N. Chintalapudi, Phys. Rev. C **52**, 1524 (1995).

[36] F. Ajzenberg-Selove, Nucl. Phys. A **529**, 1 (1991).

[37] J. A. Tostevin and J. S. Al-Halili, Nucl. Phys. A **616**, 418 (1997).

[38] A. S. Jensen and K. Riisager, Phys. Lett. B **480**, 39 (2000).

[39] Z. H. Liu, X. Z. Zhang, and H. Q. Zhang, Phys. Rev. C **68**, 024305 (2003).

[40] T. Togashi, T. Murakami, and K. Kato, Int. J. Mod. Phys. E **17**, 2081 (2008); T. Togashi, K. Kato, and T. Murakami, Int. J. Mod. Phys. A **24**, 2142 (2009).

[41] V. Lapoux *et al.*, Phys. Lett. B **658**, 198 (2008).

[42] N. Fukuda *et al.*, Phys. Rev. C **70**, 054606 (2004).